Altitude measurement using laser beam reflected from water surface

Sh. Mohammad Nejad and M. H. Haji Mirsaeidi

Abstract: In this paper altitude measurement from water surface using laser beam is presented. Research data indicate that the reflection of infrared waves from water surface is about zero and it is less than 2% for visible radiations. Phase-shift and heterodyne technique was used for the measurement, and the laser beam ($\lambda = 700nm, p = 10mW$) was modulated by a sine wave having a fixed frequency. The optimum design and low-noise elements made it possible to detect a light power about 20 nW at operating frequency.

Keywords: laser altimeter, phase shift, heterodyne technique, water surface.

1 Introduction

Altitude measurement by laser beam has a variety of applications in industry, military and navigation. The vast applications of laser altimeter are in GPS, informational and recognition satellites, altimetry for recognition and topographic planes and altimeter for cruise missiles.

There are several different methods for measuring altitudes by laser beam. A famous method called pulse, or direct time-of-flight measurement [1-2], in which the laser is derived by a narrow pulse, and the round trip time of the transmitting and receiving pulse is measured. According to the measured time, the altitude is obtained. Another method called FMCW [3], is based on frequency modulation. However, in this work, we have used the phase-shift method [4-6], the details of which will be presented hereafter.

An important parameter of measuring the altitude is the laser beam reflection from the target. The directional distribution of the radiation is also a decisive factor. The detailed explanation of these parameters and the water surface response to the laser beam will also be presented in the followings.

2 Water surface response to the laser beam

Figure 1 shows a beam, G_λ, incident on an object, which is then divided into reflection, $(G_{\lambda,ref})$, absorption, $(G_{\lambda,abs})$,and transmission, $(G_{\lambda,tr})$, rays. Therefore,

$$G_\lambda = G_{\lambda,ref} + G_{\lambda,abs} + G_{\lambda,tr} \quad (1)$$

If we denote ρ, α , and τ as the reflection, absorption and transmission coefficients respectively, then for any wavelength,

$$\rho_\lambda + \alpha_\lambda + \tau_\lambda = 1 \quad (2)$$

According to the beam reflection phenomena, surfaces are divided into two groups, namely; diffuse and specula (fig.2). Diffuse reflection happens when intensity of the reflected radiation, regardless of the direction of the incident beam, is independent of the reflection angle. However, if the whole reflection is directed toward θ_2, (which is equal to the incident angle, θ_1), the reflection is specula. Although, there is no surface to be completely diffuse or specula, however, polished and liquid surfaces are considered as nearly specula, and rough surfaces are nearly diffuse. In engineering applications however, most surfaces are assumed to be diffuse.

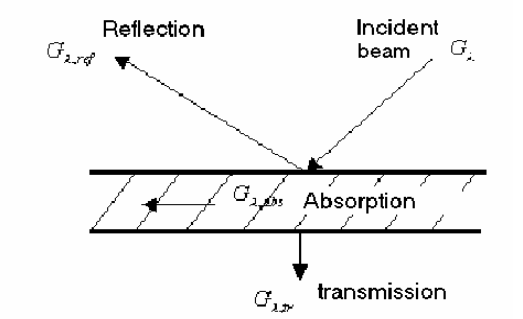

Fig. 1 Reflection, absorption and transmission of an incident beam on an object.

The presence of other materials in water also effects its properties. This is an important subject for sweet and sea waters. The sea water has a lot of unsolved salts. Although the salts do not effect the absorption spectrum, but their scattering is 30% more than the sweet water. When these materials are acted upon by a light beam, the fields and intrinsic optical properties are altered as a function of particle distribution. For any material such as water, the relation between absorption coefficient $\alpha(\lambda)$ and the imaginary part of complex index of refraction $k(\lambda)$ is,

$$\alpha(\lambda) = \frac{4\pi k(\lambda)}{\lambda} \quad (3)$$

The variation of $k(\lambda)$ with λ is shown in Figure (3). The term $n(\lambda)$ is the real part of thecomplex index of refraction. The main point is that the $k(\lambda)$ decreases from ultraviolet to visible region and then sharply increases at infrared region.

The knowledge of pure and sea water properties, allows us to distinguish between shallow and deep levels. These properties also limit the discovery and measuring by visible region of the light. Distinction of shallow water is seriously limited at green and blue regions. In other words, absorption is high at the two sides of red and blue regions. Hence, it is necessary to use green and blue lights to finding the depth.

Iranian Journal of Electrical & Electronic Engineering, 2005.
Paper first received 7th July 2003 and in revised from 11th October 2003.
Sh. Mohammad Nejad and M. H. Haji Mirsaeidi are with the Department of Electrical Engineering, Iran University of Science and Technology, Narmak, Tehran 16844, Iran.

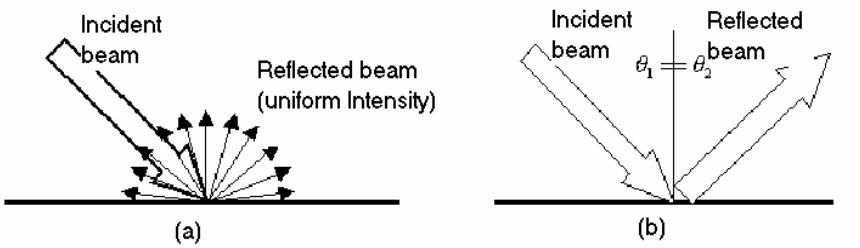

Fig. 2 Reflections, (a) diffuse, (b) specula.

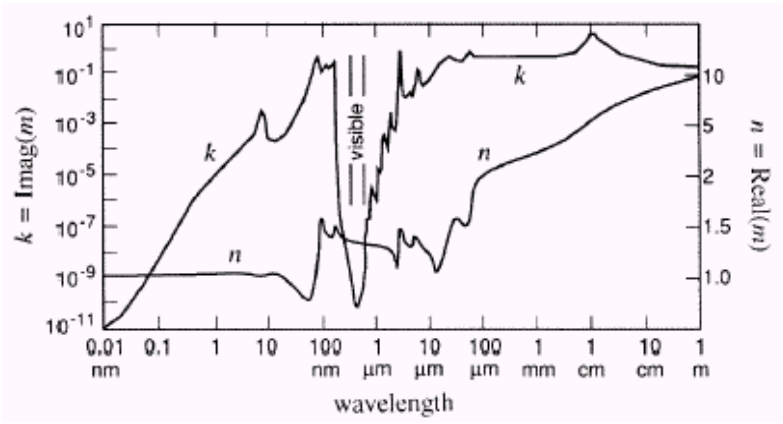

Fig. 3 Real and imaginary parts of refraction index of pure water versus wavelength [6].

The ultraviolet and infrared Reflection coefficient from water is nearly zero, and for visible light is less than 2%. Therefore, at most cases one could neglect the reflection coefficient in comparison to the absorption and transmission coefficients. Omitting ρ in equation (2) results $\alpha + \tau = 1$. The transmission coefficient for green and blue wavelengths are then maximum. Except for blue (and green) light, all other wavelengths are absorbed when passing the water depth. Since blue (and green) lights can reach to the sea bottom and reflect, one can use these wavelengths to measuring the depth. Different water categories, namely, limpid, muddy, static, wavy, deep and shallow waters have different reflection coefficients. In figure 4, full dots represent the reflection coefficients for shallow and blank ones are for deep water surfaces respectively. According to the figure, green and blue wavelengths have the highest reflections. However, in laser altimetry, green and blue wavelengths are not suitable, because in addition to the water surface reflection, they are also reflected by seabed and the resultant interference of the two reflected signals cause errors. Hence, red laser beam is the best for altimetry from water surface, and blue (or green) is suitable for water depth measurements.

Water is a specula reflector and reflects radiation at angle $180^{o} - \alpha$. Still water is a weak reflector and wavy water (such as the sea water), behaves nearly as a diffuse surface and is considered as good reflector.

Experiments prove that suspended sands will increase the reflection coefficient by 10%. This property is often used in planes and satellites to distinguish suspended objects and measure the altitudes from water surface.

In figure 5, the reflectance of different objects, including water, are given as a function of the wavelengths. It is observed that water reflectance is less than the others. Objects such as dust, plants, ice, and snow have more reflectance than water.

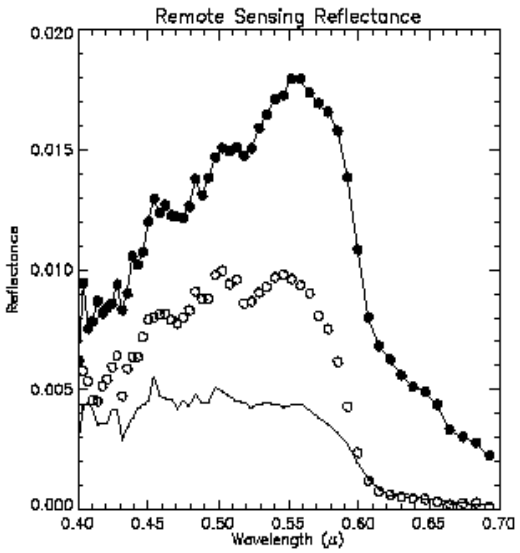

Fig. 4 Water surface reflection coefficients. Full dots are for shallow and blank ones are for deep waters, espectively [6].

3 Theoretical Discussions

In phase-shift method, the transmitted light intensity is modulated sinusoidally, and the round-trip time is turned into phase shift [4,5,7]. If f_l is the small signal modulation frequency, the phase shift is presented by,

$$\Delta\phi = \omega_l \tau_d = 2\pi f_l \frac{2d}{c} \qquad (4)$$

There are several methods of measuring the resultant phase shift [9]. In this research, because the modulation frequency is high, heterodyne technique is being employed. If s_e is the transmission (emission) signal,

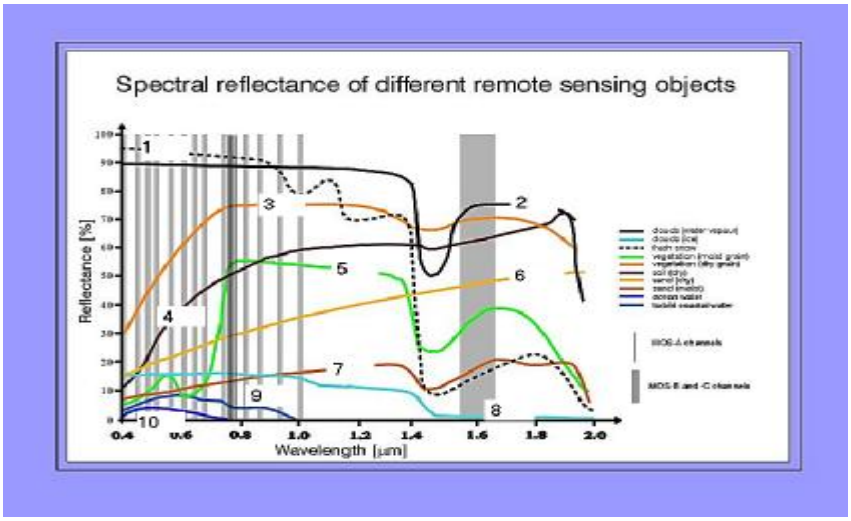

Fig. 5 Measured reflectance for different objects. 1) snow, 2) cloud, 3) dry vegetation, 4) soil, 5) green vegetation, 6) dry sand, 7) moist sand, 8) ice, 9) turbid coastal water, 10) ocean water [2].

s_r is the receiving signal, and s_2 being the reference (auxiliary) signal, then,

$$\begin{aligned} s_e &= \hat{S}_e \cos(\omega_1 t) \\ s_r &= \hat{S}_r \cos(\omega_1 t + \phi_d) \\ s_2 &= \hat{S}_2 \cos(\omega_2 t + \psi) \end{aligned} \tag{5}$$

According to these equations, it is evident that the transmitting and the receiving frequencies are equal. The term ϕ_d is the signal-phase-delay due to the round trip. The reference signal frequency is f_2 and its phase difference with the main signal is ψ. Based on the heterodyne technique, the multiplication of the transmitting and receiving signals into the auxiliary signal results,

$$\begin{aligned} X_e &= s_e.s_2 = \tfrac{1}{2}\hat{S}_e \hat{S}_2 \{\cos[(\omega_1 - \omega_2)t - \psi] \\ &\quad + \cos[(\omega_1 + \omega_2) + \psi]\} \\ X_r &= s_r.s_2 = \tfrac{1}{2}\hat{S}_r \hat{S}_2 \{\cos[(\omega_1 - \omega_2)t + (\phi_d - \psi)] \\ &\quad + \cos[(\omega_1 + \omega_2) + (\phi_d + \psi)]\} \end{aligned} \tag{6}$$

Both signals have a differentiation and addition frequencies. Using a low-pass filter to annihilate the addition part,

$$\begin{aligned} y_e &= \hat{Y}_e \cos(\omega_m t - \psi) \\ y_r &= \hat{Y}_r \cos(\omega_m t + \phi_d - \psi) \end{aligned} \tag{7}$$

where, ϕ_d (in radian) is the phase difference between the tow final signals. It is equal to that considered for the case of the round trip. Figure 6 shows the general block diagram of a phase-shift laser altimeter system, giving a primary insight to the important sections of the system.

4 Error consideration

The undesired environmental signals and noises are important error sources. The light intensity incident on photodiode has deteriorating effect on its AC parameters. Fig. 7 shows the photodiode equivalent circuit. A change of the diode's incident light intensity, will automatically change the R_{ph}, and as a result the $R_{ph}.C_{ph}$ will change. Hence, there will be a change in the phase delay $(\varphi = \arctan(RC\omega))$ of the signal. This is obviously an unwanted and undesired phase shift and an important error source.

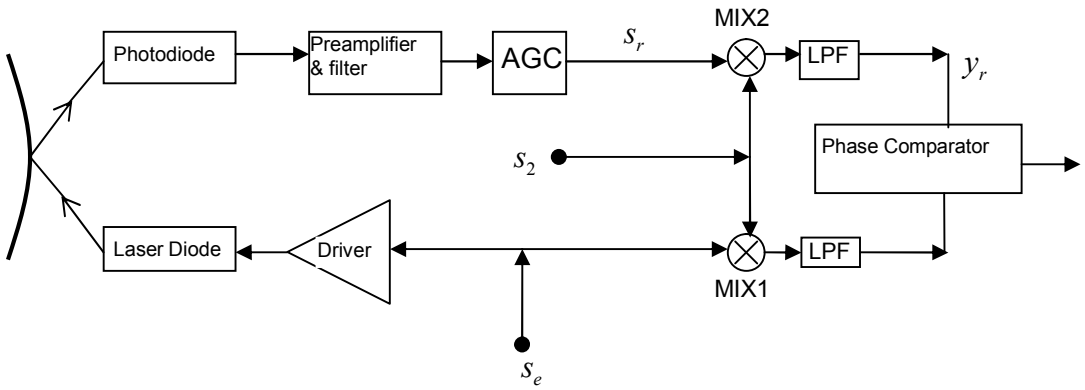

Fig. 6 The block diagram of a phase shift laser altimeter system.

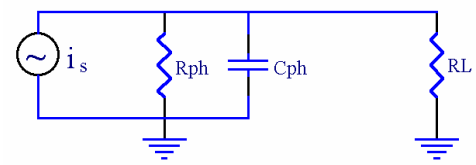

Fig. 7 The hotodiode equivalent circuit.

Crosstalk [8] is the most important error source which decreases the system precision and the maximum measurable distance. It is theoretically a signal that is electromagnetically induced on the receiver and produces error. To avoid this undesired effect, the electronic circuits of the system was shielded properly. The power sources was also isolated from other parts. This greatly eliminated the coupling between the transmitter and the receiver.

5 Electronic circuits

It is seen from fig.8 that, the circuit has a main oscillator which decides the laser's driving frequency. This is the frequency being received by the receiver. The frequency of the local oscillator ($633803\,\text{Hz}$) is chosen close to the main oscillator's frequency ($633819\,\text{Hz}$). The difference is about $16\,\text{Hz}$. The two oscillator Circuits are similar. The Produced frequencies are inputted to a divider circuit. A 1MHz bandwidth mixer is then used to mix the signals, and finally the time difference is multiplied in 30000. By introducing several delays and measuring the respected times, the relation between the altitude (L) and the measured time differences at the mixer's output becomes,

$$L = (3.4T + 0.65) \qquad (T: \text{ms}) \qquad (8)$$

In figure 8 the schematic representation of the Automatic gain control (AGC) circuit is shown. The signal is applied to the amplifier through the multiplier, and the amplifier's output is converted into DC level by *a* rms to DC converter. It is then inversed by the transistor. The transistor output voltage is again applied to the other input of the mixer, which by increasing the input amplitude, the amplifier output is increased. Hence, an increase in the converter DC level, will cause a decrease in transistor's output voltage. Multiplication of this voltage to the input signal will decreases the amplitude of the mixer output. The circuit has a perfectly fixed output amplitude for inputs ranging $0.2\text{V} \sim 7\text{V}$.

Optical receivers generally consists of two important parts, namely; the detector and the preamplifier sections. Noise elimination is one the most important task expected from a well designed preamplifier. Fig.9 presents the noise model for a transistor.

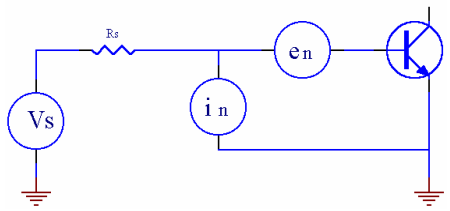

Fig. 9 Transistor noise model.

For practical sources having high output resistances, a transistor with small i_n is preferred. This will eliminate the noise voltage in the source resistance. On the other hand, if signal source has a low resistance, it's better to use a transistor having low e_n. The most important problem in designing a preamplifier circuit is an impedance that acts as a load for the photodiode. A large load resistance causes an increase of the produced signal. However, increasing the load resistance, will increase the Johnson (or thermal) noise, which in turn will effect the signal. With respect to the detector capacitance, the use of a large load causes a decrease in the high cut-off frequency. Using a low load, will also decrease the environmental light effects.

The primarily designed preamplifier circuit is shown in figure 10. Using a tank circuit as the load for the photodiode and an inductance feedback for the Op-amp, the circuit was able to detect a light power of about 200nW. In figure 11 the modified version of the circuit is presented. In this circuit an inductance load was used for the phototransistor and a tank circuit was placed as the low noise Op-amp's feedback. With this configuration, the sensitivity of the system was improved to 20nW. The sensitivity of the phototransistor used in figure 11 is about $0.5\,\text{A/W}$. The circuit was also tested using an APD having sensitivity of $20\,\text{A/W}$. In this case the detectable power was in the Pico watt ranges. However, the repeatability of the result was questionable. The experimental results are shown in table1.

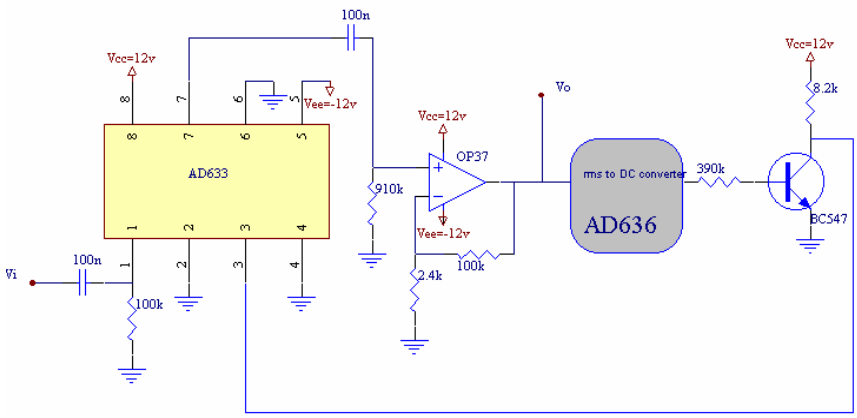

Fig. 8 Amplifier with automatic gain control circuit.

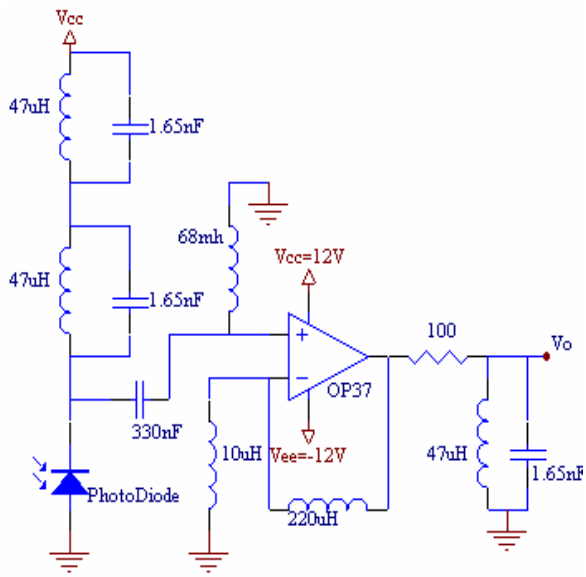

Fig. 10 Preamplifier circuit.

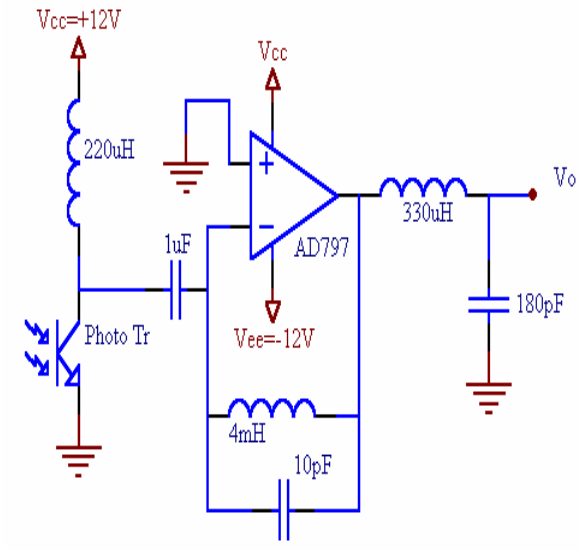

Fig. 11 Modified preamplifier circuit with high sensitivity.

Table 1 Experimental results(t is the time difference between the transmitted and received signal and T is the time difference after mixing).

t (n sec)	T (m sec)	Real Altitude (m)	Measured Altitude (m)
9	0.21	1.35	1.47
14	0.41	2.1	2.09
27	0.88	4	3.79
49	1.74	7.3	6.9
85	3.13	12.7	11.9
110	4.33	16.4	16.13
160	6.44	23.9	23.6

6 Conclusion

In this paper design and implementation of a laser-based altimeter was presented. The laser-beam-water-surface-interaction (LBWSI) experimental results for different wavelengths are also presented and analyzed. Crosstalk and environmental light effects were examined and their effects were discussed. To reduce the environmental light effects, the use of a dynamic loop in which photodiode current is held constant is proved to be appropriate. The system was tested frequently and functioned satisfactorily.

7 References

[1] L. Ramos-Izaquierdo and J. L. Bufton, "Optical System Design of the Mars Observer Laser Altimeter," Laboratory for Terrestrial Physics Goddard Space Flight Center Greenbelt, MD 20771.

[2] www.optech.on.ca/Aboutlaser.htm.

[3] B. Journet and G. Bazin,"A Low-Cost Laser Range Finder Based on an FMCW-Like Method," IEEE Transaction on Instrumentation and Measurement, Vol. 49, No. 4, 2000.

[4] B. Journet, G. Bazin and F. Bras, "Conception of an Adaptive Laser Range Finder Based on Phase Shift Measurement," Industrial Electronics, Control, and Instrumentation, Proceeding on the 1996 IEEE IECON 22nd International Conference, 1996.

[5] H. Lamela, E. Garcia, "Experimental Evaluation of Sensitivity Enhancement Achieved By Heterodyne Optical Detection In AMCW, Laser Rangefinders For Machine Vision Industrial Electronics Society," IECON '98. Proceeding on the 24th Annual Conference of the IEEE, 1998.

[6] L. Douglas Stuffle, "Bathymetry from Hyperspectral Imagry," (thesis), December, Naval Postgraguate School Montrey, California, 1996.

[7] S. Poujouly and B. Journet, " Laser Range Finder Based on Fully Digital Phase-Shift Measurement," IEEE, Dominique Miller, 1999.

[8] T. Bosch and M. Lescure, "Crosstalk Analysis of 1 m to 10 m Laser Phase-Shift Range Finder,"IEEE Transaction on Instrumentation and Measurement, Vol. 46, No. 6, 1997.

[9] s. Journet, B. Placko, "Digital Laser Range Finder: Phase-Shift Estimation by Undersampling Technique Poujouly," Industrial Electronics Society, IECON '99 Proceedings. The 25th Annual Conference of the IEEE, 1999.